# Voltammetric study of the photolysis of *fac*-tricarbonyl-$\eta^3$-{bis[2-(diphenylphosphino)ethyl]phenylphosphine}molybdenum

**Richard G. Compton,*[a] John C. Eklund,[a] Allan Hallik,[a] Sunita Kumbhat,[a] Alan M. Bond[b] and Ray Colton[b]**

[a] *Physical and Theoretical Chemistry Laboratory, South Parks Road, Oxford University, Oxford, UK OX1 3QZ*
[b] *School of Chemistry, La Trobe University, Bundoora 3083, Victoria, Australia*

Voltammetric studies at a channel electrode irradiated with monochromatic visible light have been carried out to demonstrate that the photolysis of *fac*-$Mo(CO)_3\{\eta^3$-$[(Ph_2PCH_2CH_2)_2PPh]\}$† in acetonitrile or dimethylformamide solution leads to the formation of the corresponding *mer*-isomer. No photofragmentation resulting in the loss of carbon monoxide or phosphine is observed on the voltammetric timescale. Kinetic parameters for the photo-isomerisation are reported.

A series of elegant experiments has led Davies and co-workers [1] to propose that complexes containing both phosphine and carbon monoxide ligands may preferentially lose the former on photolysis. That is, dissociative loss of CO, as is so commonly observed in metal carbonyl compounds, is not necessarily the only reaction possible. In particular a disparate series of iron complexes,[1,2] containing monodentate ligands, were shown to photofragment with the formation of free phosphine, rather than carbon monoxide, when irradiated with visible light. These conclusions were based on the successful exploitation of stereochemical techniques and phosphine exchange experiments to confirm the nature of the proposed photolytic pathway. However we have shown [2,3] that a simple, direct and quantitative approach for the study of potentially competing photofragmentation pathways arises from the adoption of voltammetric techniques in which a channel electrode is used to interrogate the identity of products formed when a solution is irradiated in its near-vicinity as shown schematically in Fig. 1. In particular, the measurement of photocurrents as a function of flow rate can be used to confirm the qualitative detail of any proposed photofragmentation mechanism and, further, to provide an estimation of its quantum yield.

In this paper we use the photo-voltammetric technique to examine the photolysis of *fac*-tricarbonyl $\eta^3$-{bis[2-(diphenylphosphino)ethyl]phenylphosphine}molybdenum, *fac*-$Mo(CO)_3\{\eta^3$-$[(Ph_2PCH_2CH_2)_2PPh]\}$, **1**. In principle, photolysis could occur by three pathways, *viz.* loss of CO, breaking of a Mo–P bond or isomerisation. Since all the metal–phosphine bonds arise only through bonding of the tridentate bis-[2-(diphenylphosphino)ethyl]phenylphosphine ligand to the molybdenum centre it might be thought exceptionally unlikely that photolysis would lead to the cleavage of all three bonds. However, dissociation of a single Mo–P bond would be likely to generate a transient pendant phosphorus ligand. A dissociative mechanism of this kind could lead to substitution by a solvent molecule or to isomerisation to the *mer*-form. Alternatively, excitation of the molecule might lead to isomerisation *via* a non-dissociative twist mechanism. *fac*-$Mo(CO)_3\{\eta^3$-$[(Ph_2PCH_2CH_2)_2PPh]\}$ therefore represents an ideal candidate molecule in which to determine whether the common preferential expulsion of carbon monoxide occurs or whether an alternative mechanism is favoured as is the case in the studies by Davies *et al.*[2]

† *fac*-$Mo(CO)_3\{\eta^3$-$[(Ph_2PCH_2CH_2)_2PPh]\}$ = (*OC*-6-22)-$Mo(CO)_3$-$\{\eta^3[(Ph_2PCH_2CH_2)_2PPh]\}$.

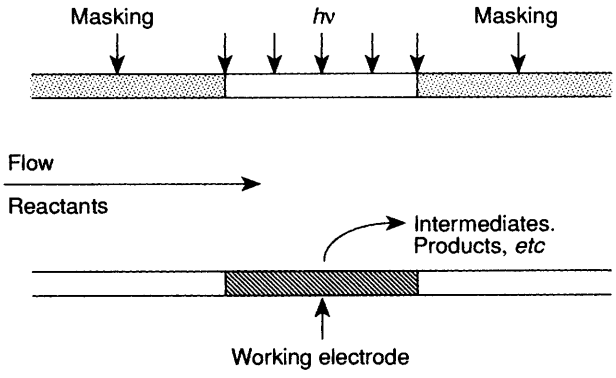


**Fig. 1** Schematic diagram of a channel electrode as used for photoelectrochemical studies

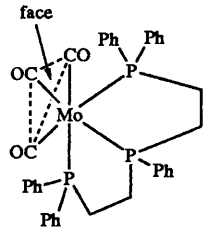


*'Fac'* isomer

## Experimental

All standard photoelectrochemical and voltammetric experiments were conducted using a platinum channel electrode made of optical quality synthetic silica to standard construction and dimensions.[2–4] Solution (volume) flow rates between $10^{-4}$ and $10^{-1}$ $cm^3$ $s^{-1}$ were employed. Working electrodes were fabricated from Pt foils (purity of 99.95%, thickness 0.025 mm) of approximate size 4 mm × 4 mm, supplied by Goodfellow Advanced Materials. Precise electrode dimensions were determined using a travelling microscope. A saturated calomel reference electrode (SCE, Radiometer, Denmark) was positioned in the flow system upstream, and a platinum gauze counter electrode located downstream, of the channel electrode. Electrochemical measurements were made using an Oxford Electrodes potentiostat modified to boost the counter electrode voltage (up to 200 V). Other methodological details were as described previously.[2–4] Irradiation was provided by a high

pressure (1000 W) xenon arc lamp (Speirs Robertson & Co. Ltd., Bedford) used in conjunction with a high intensity grating mono-chromator (maximum incident power 10 mW $cm^{-2}$) using silica lenses to focus light onto the electrode. This arrangement permitted experiments in the wavelength range 300–600 nm and also variable light intensity measurements through attenuation of the beam as described previously.[4] Complementary rotating-disc measurements were conducted using Oxford Electrodes equipment. UV–VIS measurements were made using a Perkin-Elmer Lambda-5 spectrometer.

Experiments were performed using solutions of $Mo(CO)_3\{\eta^3$-$[(Ph_2PCH_2CH_2)_2PPh]\}$ (*ca.* 0.05–0.35 mmol $dm^{-3}$) in dried[5] acetonitrile (Fisons, dried, distilled), dimethylformamide (DMF, BDH, 99%) or dichloromethane ($CH_2Cl_2$, BDH, 99.5%) solution containing 0.1 mol $dm^{-3}$ (recrystallised) tetrabutylammonium perchlorate (TBAP) (Kodak) as supporting electrolyte. Solutions were purged of oxygen by outgassing with argon that had been previously dried (calcium chloride) and then presaturated with acetonitrile prior to electrolysis. All measurements were made under thermostatted conditions at 25 °C.

### Synthesis of *fac*-$Mo(CO)_3\{\eta^3$-$[(Ph_2PCH_2CH_2)_2PPh]\}$

The method used was based on an adaptation of the borohydride method reported by Chatt *et al.*[6] and is described in detail in ref. 7.

## Results and discussion

Preliminary experiments were first performed, in the absence of light, to identify the 'dark' electrochemical behaviour of **1** at a platinum channel electrode. In acetonitrile–0.1 mol $dm^{-3}$ TBAP solution a two-electron oxidation feature was observed at a half-wave potential of +0.47 (± 0.05) V (*vs.* SCE). Cyclic voltammetry showed the oxidation to be chemically irreversible as also is the case in dichloromethane[7] where some additional details of the complete oxidation process have been elucidated. Measurements of the transport limited current as a function of the rate of flow of electrolyte solution, $V_f$, through the channel electrode demonstrated the cube root dependence expected on the basis of the Levich equation [eqn. (1)],[8] where $F$ is the

$$I_{lim} = 0.925nFD^{2/3}c_{bulk}wx_\theta^{2/3}(V_f/h^2d)^{1/3} \quad (1)$$

Faraday constant, $w$ is the electrode width, $x_\theta$ the electrode length, $d$ the channel cell width, $2h$ the cell depth, $c_{bulk}$ the bulk concentration of the electroactive species and $D$ its diffusion coefficient. A value for the diffusion coefficient of **1** was deduced: 8.0 (±0.1) × $10^{-6}$ $cm^2$ $s^{-1}$, assuming $n = 2$. Analogous behaviour was observed in DMF–0.1 mol $dm^{-3}$ TBAP solution where the half-wave potential was measured as +0.57 (±0.05) V (*vs.* SCE) and the diffusion coefficient as 3.3 (±0.4) × $10^{-6}$ $cm^3$ $s^{-1}$. The half-wave potential in dichloromethane–0.1 mol $dm^{-3}$ TBAP solution was found to be +0.48 (±0.05) V (*vs.* SCE). These 'dark' electrochemical results were checked by independent rotating-disc measurements. No quantitative experiments were conducted on dichloromethane due to associated problems of poor voltammetry and cell leakage.

Fig. 2 shows a typical hydrodynamic voltammogram recorded in acetonitrile–0.1 mol $dm^{-3}$ TBAP solution together with a corresponding voltammogram measured with the electrode irradiated using light of wavelength 330 nm and intensity of 10 mW $cm^{-2}$. It can be seen that under irradiation a new voltammetric feature with a half-wave potential of −0.25 (±0.05) V (*vs.* SCE) is observed. Corresponding experiments in DMF and dichloromethane solvents both showed light-induced pre-waves with half-wave potentials of −0.15 (±0.05) V and −0.20 (±0.05) V (both *vs.* SCE), respectively. Next an action spectrum was measured by potentiostatting the channel

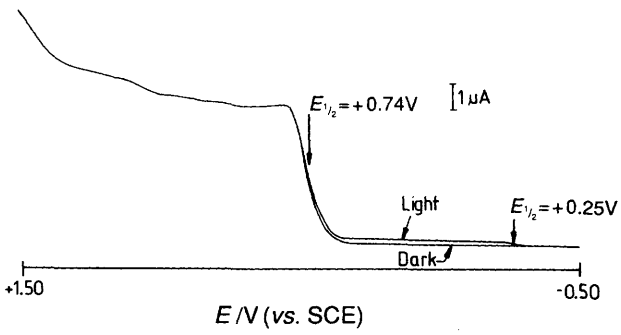


**Fig. 2** Hydrodynamic voltammogram for the oxidation of **1** in acetonitrile–0.1 mol $dm^{-3}$ TBAP solution measured at a platinum channel electrode using a flow rate of 2.3 × $10^{-3}$ $cm^3$ $s^{-1}$. Of the two traces shown one is recorded in the dark and the other in the presence of light of wavelength 330 nm.

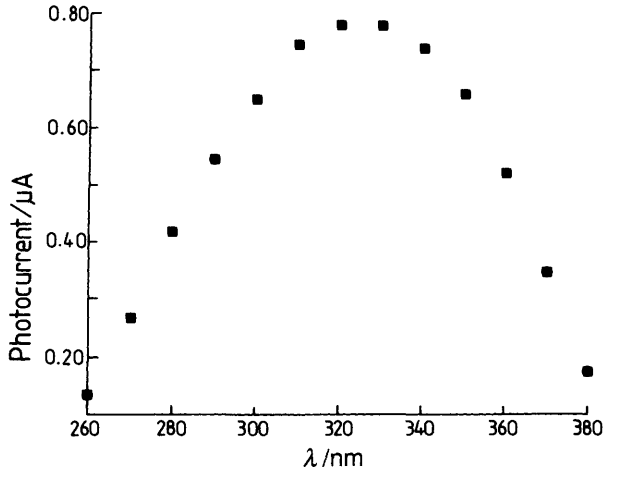


**Fig. 3** Action spectrum showing how the pre-wave photocurrent (measured at +0.05 V) varies with wavelength for the irradiation of **1** measured at a flow rate of 2.3 × $10^{-3}$ $cm^3$ $s^{-1}$ in acetonitrile–0.1 mol $dm^{-3}$ TBAP

electrode at +0.05 V (*vs.* SCE) corresponding to the transport limited oxidation of **1** and recording the photocurrent as a function of excitation wavelength at a fixed electrolyte flow rate of 2.3 × $10^{-3}$ $cm^3$ $s^{-1}$ in acetonitrile media. The result is shown in Fig. 3 which reveals that a wavelength of 330 nm corresponds to the maximum photocurrent. A similar result was observed in DMF. Since the power output of the xenon arc lamp is approximately constant over the range 300–600 nm,[3,4] the action spectrum should approximate to the absorption band responsible for inducing the photoelectrochemical activity. Accordingly UV–VIS absorption spectra were recorded of a sample of **1** dissolved in acetonitrile. This revealed bands at 208 nm ($\varepsilon$ = 32 400 $dm^3$ $mol^{-1}$ $cm^{-1}$) and 233 nm ($\varepsilon$ = 12 000 $dm^3$ $mol^{-1}$ $cm^{-1}$). The wavelength of 330 nm corresponds to a shoulder and an extinction coefficient of $\varepsilon$ = 5670 $dm^3$ $mol^{-1}$ $cm^{-1}$. The absorption characteristics in DMF are essentially unchanged; the extinction coefficient at 330 nm was measured as 5600 $dm^3$ $mol^{-1}$ $cm^{-1}$. Owing to the low value of the extinction coefficient for the shoulder at 330 nm, it is likely that the transition at 330 nm is a ligand field transition rather than a charge transfer and it is this transition that causes the resulting photoactivity of the molecule.

Next steady-state measurements of the photocurrent as a function of electrolyte flow rate were made in both acetonitrile and DMF solutions using concentrations of **1** in the range 0.05–0.33 mmol $dm^{-3}$ (acetonitrile) and 0.1–0.3 mmol $dm^{-3}$ (DMF).

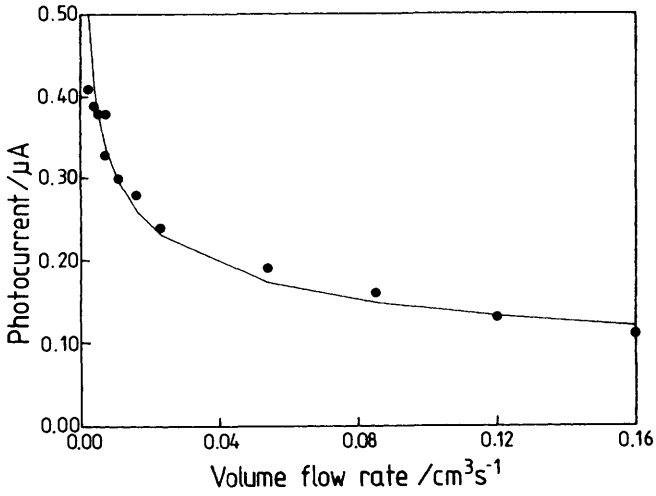


**Fig. 4** Photocurrent–flow rate data for the pre-wave associated with the illumination of **1** (0.2 mmol $dm^{-3}$) with light of wavelength 330 nm in acetonitrile–0.1 mol $dm^{-3}$ TBAP solution. The solid line represents the theoretical behaviour calculated from the model outlined in the text.

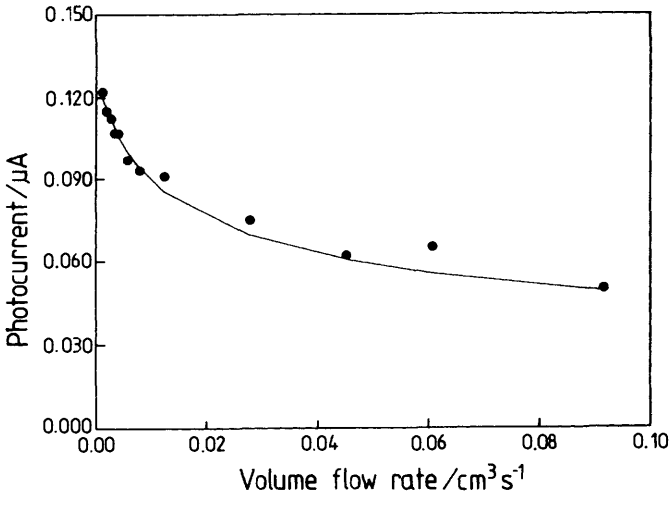


**Fig. 5** Photocurrent–flow rate data for the pre-wave associated with the illumination of **1** (0.2 mmol $dm^{-3}$) with light of wavelength 330 nm in DMF–0.1 mol $dm^{-3}$ TBAP solution. The solid line represents the theoretical behaviour calculated from the model outlined in the text.

Typical results are shown in Figs. 4 and 5. For all concentrations of **1** a steady decrease of the absolute photocurrent with flow rate was observed. Also the ratio of the pre-wave photocurrent to that of the parent oxidation wave measured in the dark was found to decrease systematically with flow rate. This is indicative[2-4] of light being absorbed by the parent compound before electrolysis, as opposed to absorption by a post-electrolysis product, and this observation together with the inferences made from the action spectra data given above, led to the following models being proposed for the photooxidation (in acetonitrile).

*Model A: photofragmentation to CO.*—

$$fac\text{-}Mo(CO)_3\{\eta^3\text{-}[(Ph_2PCH_2CH_2)_2PPh]\} + h\nu \longrightarrow CO + Mo(CO)_2\{\eta^3\text{-}[(Ph_2PCH_2CH_2)_2PPh]\}(CH_3CN) \quad (i)$$

$$Mo(CO)_2\{\eta^3\text{-}[(Ph_2PCH_2CH_2)_2PPh]\}(CH_3CN) - ne^- \longrightarrow \text{products} \quad (ii)$$

*Model B: photofragmentation to phosphine.*—

$$fac\text{-}Mo(CO)_3\{\eta^3\text{-}[(Ph_2PCH_2CH_2)_2PPh]\} + h\nu \longrightarrow (Ph_2PCH_2CH_2)_2PPh + Mo(CO)_3(CH_3CN)_3 \quad (iii)$$

$$Mo(CO)_3(CH_3CN)_3 - ne^- \longrightarrow \text{products} \quad (iv)$$

*Model C: photoisomerisation.*—

$$fac\text{-}Mo(CO)_3\{\eta^3\text{-}[(Ph_2PCH_2CH_2)_2PPh]\} + h\nu \longrightarrow mer\text{-}Mo(CO)_3\{\eta^3\text{-}[(Ph_2PCH_2CH_2)_2PPh]\} \quad (v)$$

$$mer\text{-}Mo(CO)_3\{\eta^3\text{-}[(Ph_2PCH_2CH_2)_2PPh]\} \longrightarrow fac\text{-}Mo(CO)_3\{\eta^3\text{-}[(Ph_2PCH_2CH_2)_2PPh]\} \quad (vi)$$

$$mer\text{-}Mo(CO)_3\{\eta^3\text{-}[(Ph_2PCH_2CH_2)_2PPh]\} - ne^- \longrightarrow \text{products} \quad (vii)$$

*Model D: photosubstitution.*—

$$fac\text{-}Mo(CO)_3\{\eta^3\text{-}[(Ph_2PCH_2CH_2)_2PPh]\} + h\nu \longrightarrow Mo(CO)_3\{\eta^2\text{-}[(Ph_2PCH_2CH_2)_2PPh]\}(CH_3CN) \quad (viii)$$

$$Mo(CO)_3\{\eta^2\text{-}[(Ph_2PCH_2CH_2)_2PPh]\}(CH_3CN) - ne^- \longrightarrow \text{products} \quad (ix)$$

Note that the photoisomerisation process might occur either dissociatively or through a non-dissociative twist mechanism. It has also been assumed that the oxidation of the *mer* species, like the *fac*, proceeds *via* an overall irreversible two electron mechanism under the conditions employed.

The models were first examined by deciphering the signatures written in the photo-voltammograms such as that displayed in Fig. 2. In all experiments the only two voltammetric features observed in the presence of light in the voltage range −2.0 to +2.0 V were that from the (unreacted) parent material at half-wave potentials identical to those seen in the dark and that from the single pre-wave seen close to −0.20 V (*vs.* SCE) regardless of solvent, flow rate or light intensity. These observations are inconsistent with Model B since this would lead to voltammetric features with half-wave potentials attributable to both a free phosphine (typically close to +1.50 V[2]) and free $Mo(CO)_3(CH_3CN)_3$ (reported as +0.15 V[3c]). Thus photofragmentation into free phosphine can be eliminated as a possible mechanism. Next we compare Models A and D with Model C and note that whereas Models A and D would produce different electroactive photoproducts according to the medium employed, since a solvent molecule is incorporated into the molybdenum species to replace the photo-ejected carbon monoxide, it is the case that Model C would produce an identical species, the *mer*-isomer, regardless of the solvent system. Since almost identical half-wave potentials are seen for the pre-wave in the three different solvents, acetonitrile, DMF and dichloromethane, studied, this strongly suggests the operation of pathway C. Towards confirmation of this we note that since the solution contains neither free phosphine nor free CO an irreversible photochemical step cannot be reversed thermally back to the parent material in the case of Models A or B. Accordingly step (*vi*) has been included in Model C in the scheme given above. Since the absence or presence of a thermal reversion of the photochemical step provides a kinetic method for distinguishing Models A (and B) from Model C we next consider the kinetic analysis of the photo-current/flow rate data of Figs. 4 and 5 in the light of the reaction mechanisms proposed. These were modelled treating the first-order rate constants, $k_{(i)}$ and $k_{(v)}$, for the light induced steps (*i*) and (*v*) as adjustable parameters. In the case of Model C the thermal reversion rate constant, $k_{(vi)}$, was treated similarly. The diffusion

**Table 1**

| Solvent | $D/10^{-6}$ cm$^2$ s$^{-1}$ | $\varepsilon^a$/dm$^3$ mol cm$^{-1}$ | $k_{(v)}/10^{-3}$ s$^{-1}$ | $k_{(vi)}$/s$^{-1}$ | $\Phi^a$ |
|---|---|---|---|---|---|
| $CH_3CN$ | 8.0 (± 1.0) | 5670 | 6.0 (± 2.0) | 0.0 (± 0.05) | 0.015 (± 0.005) |
| DMF | 3.3 (± 0.4) | 5600 | 5.2 (± 2.0) | 0.20 (± 0.10) | 0.015 (± 0.005) |

[a] Measured at a wavelength of 330 nm.

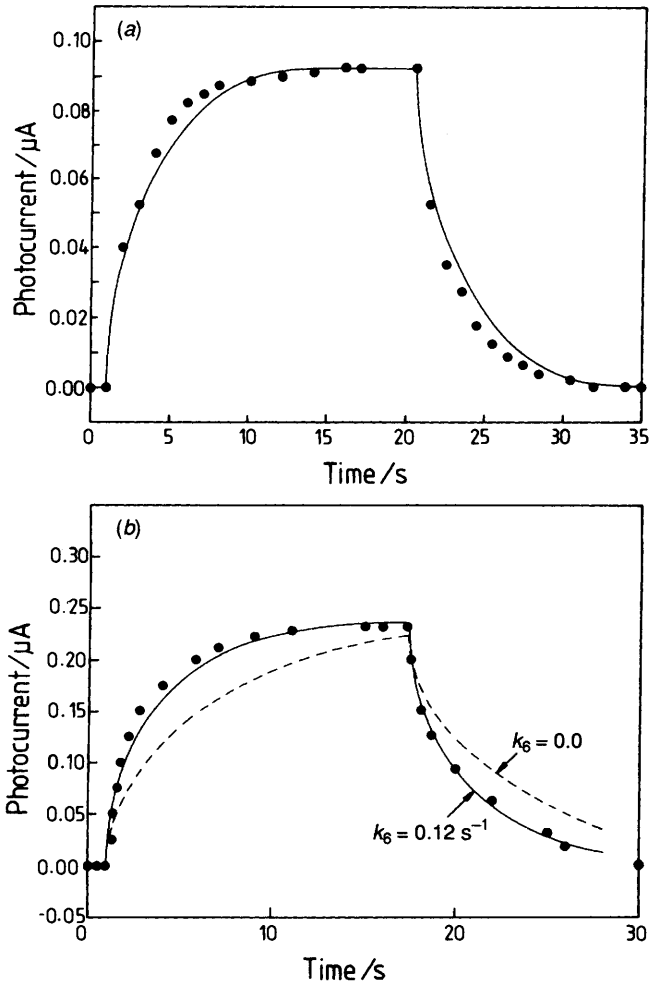


**Fig. 6** Experimental phototransients (●) recorded at a light intensity of 10 mW cm$^{-2}$ for the oxidation of **1** at a flow rate of 2.3 × 10$^{-3}$ cm$^3$ s$^{-1}$. Plot (*a*) was recorded using acetonitrile as solvent with $c_{bulk}$ = 0.1 mmol dm$^{-3}$. Plot (*b*) was recorded using DMF as solvent with $c_{bulk}$ = 0.3 mmol dm$^{-3}$. The solid lines are the theoretically predicted transients computed using the kinetic parameters deduced from the steady-state photocurrent-flow rate data (see Table 1). The dashed line in plot (*b*) shows the effect of putting $k_{(vi)}$ equal to zero in the modelling and clearly demonstrates the requirement for a thermal back reaction in the case of DMF as solvent.

coefficient of the electroactive species in each case, $Mo(CO)_2\{\eta^3$-$[(Ph_2PCH_2CH_2)_2PPh]\}(CH_3CN)$ and *mer*-$Mo(CO)_3\{\eta^3$-$[(Ph_2PCH_2CH_2)_2PPh]\}$, was approximated by the measured value for **1** in the appropriate solvent medium. The basis for this is the Wilke–Chang empirical correlation for predicting diffusion coefficients which suggests that the likely error will at the most be 10%.[9] The necessary theory for computing the theoretical behaviour for the proposed model, or any other chemical scheme, is well established and the interested reader is directed towards the literature for the necessary details.[10] No new computational or conceptual problems emerge in their application to the present work. The experimental data, as shown in Figs. 4 and 5, was found to be consistent only with the choice of Model C, but not Model A (and thus B), when the data in both solvents was considered. Note that, kinetically, Model D with a first-order thermal back reaction is also consistent with the results of the modelling. However, the reasons for discounting Model D, namely the insensitivity of the oxidation potential of the pre-wave to solvent type, were given above.

Specifically the data obtained in DMF solution required the existence of a first-order thermal reversion of the electro-active photoproduct for satisfactory agreement between theory and experiment to be obtained over the entire range of electrolyte flow rates studied. The level of agreement seen for Model C may be judged from Figs. 4 and 5, which in addition to the experimental data, show the theoretically computed behaviour calculated using the best fit parameters shown in Table 1. These kinetic inferences were independently verified by means of photo-transient experiments[11] in which the electrode was potentiostatted at a value (+0.20 V *vs.* SCE) corresponding to the transport limited current for the oxidation of the electro-active photoproduct and then the evolution of the photocurrent in time monitored after the pulsewise application of light to the system. It is possible to compute the expected transient response as a function of flow rate using Model C and the values for kinetic parameters given in Table 1 as deduced from the steady-state experiments. Typical results for both acetonitrile and DMF as solvents are shown in Fig. 6 together with the experimentally recorded phototransient. The good agreement between theory and experiment serves to confirm the mechanism proposed and the values of the parameters inferred from the steady-state experiments.

Examination of Fig. 6(*b*) in which the computed theoretical transient is compared with the experimental, with both the thermal back reaction included and excluded, serves to demonstrate the need for this reaction in DMF as solvent. The question arises as to why this process is only observed in DMF, but not in acetonitrile. The key point is that the kinetic processes observable in our experiments are only those which take place on the voltammetric timescale. This reflects not only the electrode size and the flow rate used, but also the rate of diffusion in the medium employed.

DMF is significantly more viscous than acetonitrile as reflected in the relative diffusion coefficients of **1** measured in the two media. The consequence of this is that the photovoltammetric experiments are slightly more sensitive to slow kinetic events in DMF compared with acectonitrile. Physically this is because the electroactive photoproduct has less tendency to escape from the electrode surface in the case of DMF. Thus the fact that no back reaction is discernible in acetonitrile simply means that its rate constant is less than 0.05 s$^{-1}$.

Finally, we note that the kinetic and absorption data in Table 1 permit the inference of the quantum yield for the photoisomerisation reaction at the wavelength used (330 nm). The result is a value of 0.015 for both acetonitrile and DMF solvents. The insensitivity of this value to the medium employed again provides further evidence in favour of Model C over Models A, B or D. Also, it is instructive to compare the results obtained above with those measured using cyclic voltammetry under fast scan conditions in $CH_2Cl_2$ where the oxidation of the *fac*-isomer simplifies to a one electron process.[7] In that situation, a square reaction scheme is operative and potential

data for the presumed reversible one-electron oxidation of the *mer*-isomer is obtained. Calculations reveal that the *mer*-isomer is easier to oxidise than the *fac*-isomer by *ca.* 250 mV.[7] In the work described above the oxidation of the presumed *mer*-isomer also is more positive, but by an amount greater than 250 mV. However the oxidation (two electron) of the *mer* species in the present study is not a reversible process, nor is the oxidation of the *fac*-isomer. The different mechanisms applying to the processes imply that direct comparisons of potentials are not appropriate. In contrast when photoisomerisation of a manganese carbonyl complex was reported direct comparisons of potential were appropriate.[3e]

## Conclusions

Photo-voltammetry has shown that the photolysis of *fac*-$Mo(CO)_3\{\eta^3$-$[(Ph_2PCH_2CH_2)_2PPh]\}$ leads not to the ejection of carbon monoxide, but probably to isomerisation to the *mer*-form either *via* a twist mechanism or through partial dissociation of the phosphine although photosubstitution (Model D) with a thermal reversion reaction is not absolutely ruled out. As such these observations provide an extension to the ideas of Davies and co-workers,[1] excitation of metal complexes containing carbon monoxide and a monodentate phosphine ligand need not induce loss of CO on photolysis. In the present case with a tridentate phosphine, CO also is not lost, but the preferred reaction is isomerisation (or photosubstitution).

## Acknowledgements

We thank the EPSRC (Grant No. GR/H99288) for financial support and for a studentship for J. C. E., The Australian Research Council for financial support, The Royal Society for supporting A. H. under the FSU Joint Projects Scheme and the Association of Commonwealth Universities for an Academic Staff Fellowship for S. K.

## References

1 (*a*) S. G. Davies, M. R. Metzler, K. Yanada and R. Yanada, *J. Chem. Soc., Chem. Commun.*, 1993, 658; (*b*) S. G. Davies and W. C. Watkins, *J. Chem. Soc., Chem. Commun.*, 1994, 491.

2 (*a*) S. G. Davies, M. R. Metzler, W. C. Watkins, R. G. Compton, J. Booth and J. C. Eklund, *J. Chem. Soc., Perkin Trans. 2*, 1993, 1005; (*b*) S. G. Davies, M. R. Metzler, W. C. Watkins, R. G. Compton, J. Booth and J. C. Eklund, *J. Chem. Soc., Perkin Trans. 2*, 1993, 1603.

3 (*a*) R. G. Compton, R. Barghout, J. C. Eklund, A. C. Fisher, S. G. Davies and M. R. Metzler, *J. Chem. Soc., Perkin Trans. 2*, 1993, 39; (*b*) R. G. Compton, J. Booth and J. C. Eklund, *J. Chem. Soc., Dalton Trans.*, 1994, 1711; (*c*) R. G. Compton, R. Barghout, J. C. Eklund and A. C. Fisher, *Electroanalysis*, 1994, **6**, 45; (*d*) R. G. Compton, R. Barghout, J. C. Eklund, A. C. Fisher, S. G. Davies, M. R. Metzler, A. M. Bond, R. Colton and J. N. Walter, *J. Chem. Soc., Dalton Trans.*, 1993, 3641; (*e*) R. G. Compton, R. Barghout, J. C. Eklund, A. C. Fisher, A. M. Bond and R. Colton, *J. Phys. Chem.*, 1993, **97**, 1661.

4 (*a*) R. G. Compton, R. A. W. Dryfe and A. C. Fisher, *J. Chem. Soc., Perkin Trans. 2*, 1994, 1581; (*b*) R. G. Compton, R. A. W. Dryfe and A. C. Fisher, *J. Electroanal. Chem.*, 1993, **361**, 275; (*c*) R. G. Compton, R. G. Wellington, A. C. Fisher, D. Bethell and P. Lederer, *J. Phys. Chem.*, 1991, **95**, 4749.

5 J. F. Coetzee, *Recommended Methods for Purification of Solvents*, IUPAC, Pergamon Press, Oxford, 1982.

6 J. Chatt, G. J. Leigh and N. J. Thankarajan, *J. Organometallic Chem.*, 1971, **29**, 105.

7 A. M. Bond, R. Colton, S. W. Feldberg, P. J. Mahon and T. Whyte, *Organometallics*, 1991, **10**, 3320.

8 V. G. Levich, *Physiochemical Hydrodynamics*, Prentice-Hall, Englewood Cliffs, New Jersey, 1962.

9 C. R. Wilke and P. Chang, *A. I. Ch. Eng. Journal*, 1955, **1**, 261.

10 (*a*) A. C. Fisher and R. G. Compton, *J. Phys. Chem.*, 1991, **95**, 7538; (*b*) A. C. Fisher and R. G. Compton, *J. Appl. Electrochem.*, 1992, **22**, 38; (*c*) R. G. Compton, M. B. G. Pilkington and G. M. Stearn, *J. Chem. Soc., Faraday Trans. 1*, 1988, **84**, 2155.

11 R. G. Compton, R. A. W. Dryfe and J. Hurst, *J. Phys. Chem.*, 1994, **98**, 10 497.

*Paper* 5/00792E
*Received* 9*th February* 1995
*Accepted* 7*th March* 1995